AD-A251 085

OFFICE OF NAVAL RESEARCH

Grant N00014-90-J-1971

R&T Code 4131001 phy

Technical Report No. 5

Vibrationally Induced Rotational Axis Switching: A Novel Mechanism for Vibrational Mode-Coupling

by

H. Li, Gregory S. Ezra, and Laura A. Philips

Submitted for Publication
in the
Journal of Chemical Physics

Cornell University
Department of Chemistry
Ithaca, NY 14853-1301

May 29, 1992

DTIC
ELECTE
JUN 0 5 1992
S B D

Reproduction in whole or in part is permitted for any purpose of the United States Government

This document has been approved for public release and sale; its distribution is unlimited.

92-14658

92 6 03 058

Submitted J. Chem. Phys

VIBRATIONALLY INDUCED ROTATIONAL AXIS SWITCHING: A NOVEL MECHANISM FOR VIBRATIONAL MODE-COUPLING

H. Li, Gregory S. Ezra, and Laura A. Philips,
Department of Chemistry, Cornell University, Ithaca, NY 14853-1301

Abstract

High resolution IR spectra of small- to medium-sized molecules such as 2-fluoroethanol (2FE) show that the effective density of coupled states is often greater than that obtained by a direct count of vibrational states. A novel mechanism for rotation-vibration interaction, vibrationally induced rotational axis switching (VIRAS), is proposed as a possible explanation for these discrepancies. VIRAS has its origin in centrifugal distortion, and is physically distinct from Coriolis coupling. In the case of 2FE, we explicitly treat the coupling of overall rotation with large-amplitude internal rotation about the C-C bond. Assuming a uniform coupling of all dark vibration-torsion states to the bright state, we predict a density of coupled states in good agreement with that observed in the C-H stretching region at 2980 cm^{-1}.

I. INTRODUCTION

Intramolecular vibrational energy redistribution (IVR) has been the focus of intensive work, both theoretical and experimental, over the past decade.[1-21] The idea of state-selective laser excitation to control chemical reaction rates has been the motivation for a variety of experiments. One would like to mode-selectively excite a molecule to obtain reaction rates or product distributions that are functions of the particular mode excited, rather than just the total energy and angular momentum. Rapid IVR is, however, a major obstacle to such dreams. Factors influencing rates and mechanisms of IVR are varied and extensive, and not as yet completely understood. As a result, both experimentalists and theorists continue striving to understand the phenomenon of IVR.

The consequences of IVR are manifest in both time-domain and frequency-domain experiments.[1-14] Frequently, IVR is viewed as an explicitly

time-dependent phenomenon, in which a non-stationary state is initially prepared and evolves in time. Energy flows out of the initially excited mode, which may be localized in one part of the molecule, to other modes and, consequently, other parts of the molecule. The nonstationary state initially prepared is often referred to as the "bright state", as it carries oscillator strength for the spectroscopic transition of interest, and IVR results in the flow of amplitude into the manifold of so-called "dark states" that are not excited directly. It is of interest to understand what physical interactions couple different modes, allowing energy to flow between them. In contrast to time-domain measurements, experiments in the frequency domain excite eigenstates of the molecule, which do not evolve with time. Splittings and perturbations observable in high resolution spectra can yield detailed information on the amount of mode-coupling in a given molecule. The molecular eigenstates can be described as a superposition of zeroth-order states that would be excited in the corresponding time-domain experiments. Conversely, time-domain experiments may be analyzed in terms of the preparation of superposition states of the molecular eigenstates. Once again, we would like to predict which bright and dark states couple and what physical mechanism causes such coupling.

Various mechanisms that have been invoked to explain vibrational mode-coupling include anharmonic, centrifugal and Coriolis coupling. Each coupling mechanism has been successfully employed to account for mode-coupling in different circumstances.[4-10] For example, anharmonic coupling is independent of rotational angular momentum and therefore only directly couples states with the same angular momentum quantum numbers. Both centrifugal and Coriolis coupling terms are dependent on angular momentum and will therefore depend on the rotational level of the

molecule. For example, Kommandeur et al. analyze both time and frequency resolved data and discuss in detail the application of these mechanisms to mode-coupling in the mid-sized molecule pyrizine.[10] From these as well as other experiments[4-13], it is clear that rotational angular momentum can play an important role in state mixing, and our understanding of the physical mechanism of rotation dependent vibrational mode-coupling is far from complete.

High resolution vibrational spectroscopy has been used to resolve individual ro-vibrational eigenstates in molecules of intermediate size.[4-8] Perturbations in the spectra of many molecules lead to the appearance of clusters of peaks where one would expect to see a single ro-vibrational transition. These clusters or clumps of peaks are direct evidence of state coupling. Each additional peak in such a clump of peaks represents mixing of the bright state with a dark state. Such spectral features have been observed in a number of studies of mid-sized organic molecules in molecular beams.[4-8] In some cases, there is a rotational dependence to the mode-coupling,[6-8] while in others the mode coupling is independent of rotation.[5,6] In either case, there is often a discrepancy between experiment and theory in the number of coupled states.

One approach used to determine the mechanism of vibrational coupling is to compare the theoretically predicted density of coupled states to the density of coupled states measured experimentally. Using a zeroth-order basis set of bright and dark states, the total number of vibrational states available to couple to the bright state is estimated from the calculated density of dark states in the spectral region of interest. In the absence of rotation-vibration coupling, this total density of vibrational states should give an upper bound for the number of coupled states, since all dark states will not

DTIC INSPECTED

For
n
n/
ity Codes
Dist Avail and/or Special
A-1

necessarily couple to the bright state. Experimentally, the density of coupled states is inferred from the number of transitions in a clump of peaks in the spectrum. The spacing of the dark states as calculated from the spacing of the transitions in the spectrum is a measure of the density of states actually coupled to the bright state.[5-8] In all of the experiments cited above the experimental density of coupled states is larger than the calculated density of states. This discrepancy can be explained if, for example, a single ro-vibrational bright state is able to couple to more than one rotational state associated with each of the vibrational dark states. Such coupling may occur via the Coriolis mechanism [22,23]. Coriolis coupling alone, however, does not always account for the observed discrepancy between experiment and theory. As a result, other variations and combinations of Coriolis coupling and anharmonic coupling have been proposed.[5,6,9,15] We analyze here an alternate mechanism, physically distinct from Coriolis coupling, whereby a single ro-vibrational bright state can couple to more than one ro-vibrational dark state. The mechanism considered is a consequence of centrifugal coupling, and has a straightforward physical interpretation in terms of vibrationally induced changes in the orientation of the principal axes.

Recent work in our laboratory on the high resolution spectroscopy of 2-fluoroethanol (2FE) has motivated our interest in coupling mechanisms[7,8]. In the C-H stretching region of 2FE at 2980 cm^{-1}, extensive mode-mode coupling has been observed. The experimental density of coupled states is determined to be 200-250 states/cm^{-1}. The density of *vibrational* states in the neighborhood of 2980 cm^{-1} estimated on the basis of a simple rigid rotor/harmonic oscillator/hindered rotor model is between 35 and 58 states/cm^{-1}, depending on the potential functions used in the calculation. In this calculation the fundamental vibrational frequencies for all but the

torsional modes, were used from experimental measurements[25], and a 2% anhamonicity was assumed. The torsional modes were treated as hindered rotors.[26] An additional coupling mechanism is apparently required to account for the discrepancy between experiment and calculation.

One possible coupling mechanism that will lead to rovibrational mixing is standard Coriolis coupling. The Coriolis term in the Watson Hamiltonian[22] directly couples zeroth-order vibrational states differing bt one quantum in each of two modes. As dark states in 2FE at approximately 3000 cm^{-1} contain as many as 80 quanta, it is necessary to invoke very high order combinations of anharmonic and Coriolis perturbations to explain the observed level density. The observed J-dependence of the density of coupled states is, however, relatively weak (see Fig. 7), suggesting that Coriolis coupling is significant only to low order, if at all. We are therefore led to examine additional rotation-vibration coupling mechanisms to explain the perturbations observed in the high resolution infrared spectrum of 2FE. In this paper, we analyze a mechanism for rovibrational mixing based on the phenomenon of vibrationally induced rotational axis switching (VIRAS). VIRAS is most pronounced for dark states containing torsional modes, where large-amplitude internal rotation occurs.

A summary of the paper follows: in Section II we introduce the key physical idea of VIRAS in the context of the conventional description of rotation-vibration interaction in semi-rigid molecules. The theory is then developed in more detail for a molecular model in which one large-amplitude internal motion is treated explicitly. In Section III we apply the theory to 2FE. The VIRAS mechanism is able to provide a very reasonable estimate for the density of states coupled to a given bright state for the example of 2FE. Conclusions are given in Section IV.

II. THEORETICAL APPROACHES TO ROTATION-VIBRATION COUPLING

In this Section we first introduce the essential physical idea of vibrationally induced rotational axis switching in the simple context of the usual rotation-vibration Hamiltonian for semi-rigid molecules. To apply the theory to the particular case of 2FE, however, it is necessary to consider explicitly large-amplitude torsional motion.

A. Bright and Dark States

The standard spectroscopic approach to the problem of vibration-rotation coupling in semi-rigid molecules involves calculation of the eigenvalues and eigenvectors of the Watson Hamiltonian for small amplitude motion.[22] The zeroth-order solution to the vibration-rotation problem is based on the harmonic-oscillator/rigid rotor separation of vibration and rotation. The vibrational modes are treated as a set of independent harmonic oscillators and the rotational states are taken to be eigenstates of a rigid asymmetric top. The corresponding zeroth-order Hamiltonian has the usual form for nonlinear semi-rigid molecules:

$$H^0 = \frac{1}{2}\sum_k P_k^2 + U(Q) + AJ_A^2 + BJ_B^2 + CJ_C^2 \qquad \text{[Eq. 1]}$$

where it is assumed that the Eckart frame is aligned with the principal axes of the inertia tensor at the equilibrium configuration (zero vibrational displacement). P_k is the momentum conjugate to the k^{th} normal vibration and U(Q) is the potential energy for
(3N-6) independent harmonic oscillators. Eigenfunctions of H^0 are products $|\{n_j\}>|J,\lambda>$ of the 3N-6 harmonic oscillator wavefunctions $|\{n_j\}>$, where $\{n_j\}$ is a set of vibrational quantum numbers for the 3N-6 modes of the molecule, and asymmetric rotor wavefunctions $|J,\lambda>$, where λ is a book-keeping label

that serves to distinguish between the 2J+1 states of the same total rotational angular momentum J. These zeroth-order wavefunctions are often taken to describe the bright state and dark states in time-resolved experiments at low levels of excitation[9]. Transition probabilities may be derived based on properties of these states.

Coupling terms are obtained by subtracting H^o from the full Watson Hamiltonian. Anharmonic coupling terms depend only on vibrational variables, while Coriolis and centrifugal coupling terms depend on both vibrational and rotational variables. Due to the presence of these coupling terms, the functions $|\{n_j\}>|J,\lambda>$ are no longer eigenstates of the full rovibrational Hamiltonian. Nevertheless, the zeroth-order states $|\{n_j\}>|J,\lambda>$ serve as a complete basis set in which to expand the true rotation-vibration eigenstates, $|\Psi,J>$:

$$|\Psi,J>=\sum_{\{n_j\},\lambda'} C_{\{n_j\},\lambda'}|\{n_j\}>|J,\lambda'> \qquad \text{[Eq. 2]}$$

A "bright state" is a particular zeroth-order state $|\{n_j\}>|J,\lambda'>$ that carries oscillator strength for a given spectroscopic transition in the harmonic-oscillator/rigid-rotor approximation. If the bright state contributes significantly to several molecular eigenstates $|\Psi,J>$, one will see more transitions in the experimental spectrum than predicted by a calculation based on the rigid rotor, harmonic oscillator model. The bright state/dark state picture becomes less useful when the molecular eigenstates have significant admixtures of several bright states, producing a spectrum that is unassignable in terms of the zeroth-order quantum numbers.

Different coupling mechanisms will mix different types of zeroth-order states in $|\Psi,J>$. For example, anharmonic coupling terms, which involve only vibrational variables, will only mix directly different $\{n_j\}$'s, while the rotational part $|J,\lambda>$ remains unaffected.
Both centrifugal and Coriolis coupling also mix different $|J,\lambda>$'s, but total J must, of course, be conserved. Coriolis coupling or centrifugal coupling plus anharmonic coupling can mix, in principle, all of the rotational states associated with any two vibrational states.

The physical origin of Coriolis coupling is the interaction of molecular rotation with the vibrational angular momentum induced by the simultaneous excitation of a pair of vibrational modes. For example, in the case of a linear triatomic molecule, Coriolis interactions can couple the asymmetric stretch and the bend. As the vibrating molecule rotates, there is a Coriolis force on each nucleus proportional to the vector product of its momentum with the angular velocity vector. For the asymmetric stretch mode, the combination of forces on the individual nuclei results in excitation of a component of bending motion. The effects of Coriolis coupling are most pronounced when the two modes have nearly equal frequencies.

Centrifugal coupling arises from the vibrational coordinate dependence of the molecular moments of inertia. In the VIRAS mechanism we focus attention on a rotation-vibration coupling phenomenon that is a consequence of centrifugal interaction, and so is physically distinct from Coriolis coupling. This VIRAS phenomenon is analogous to axis switching in electronic transitions[25].

B. Vibrationally Induced Rotational Axis Switching in Semi-rigid Molecules

To introduce the VIRAS phenomenon for semi-rigid molecules, consider an adiabatic separation of (3N-6) "fast" vibrations from "slow" rotation. Each vibrational state then has an effective rotational Hamiltonian obtained by averaging over the vibrational coordinates, and anharmonic couplings will couple different zeroth-order vibrational states. The bright vibrational state is defined as the product of an appropriate excited vibrational state with an eigenstate of the associated rotational Hamiltonian. In general, rotational constants and, most importantly, the *orientation* of principal inertial axes (with respect to the Eckart frame) will be different for different vibrational states. The change in orientation of the inertial axes with vibrational state is called vibrationally induced rotational axis switching (VIRAS).

Suppose for the moment that the molecular Hamiltonian contains only anharmonic perturbations, which serve to mix vibrational states. The dependence of rotational constants and principal axis orientation on vibrational state then implies that the bright state is coupled to a dark state that has principal axes rotated with respect to the principal axes of the bright state. Since the asymmetric top quantum numbers refer to a specific orientation of the principal axes, if the axes are rotated, the asymmetric top quantum numbers are no longer conserved. The result is that a given rotational bright state, with given angular momentum quantum numbers, can in fact couple via anharmonic perturbation to several rotational states associated with a particular dark vibrational state. That is, VIRAS results in a breakdown of rotational "selection rules", just as in the analogous phenomenon for electronic transitions.

The amount of rotational mixing is of course a function of vibrational state. Vibrational modes which induce the largest changes in both rotational constants and orientation of the principal axes are likely to have the most dramatic rotational state mixing via VIRAS. In particular, vibrational modes involving large-amplitude low frequency torsional motion will cause considerable changes in molecular geometry and concomitant changes in rotational constants and principal axis orientation. For example, we expect the torsional modes in 2FE to have the largest VIRAS effect (see next Section). As an example, shown in Figure 1 is a diagrammatic representation of the reorientation of the principal axes for two different vibrational dark states of 2FE, one containing no torsion and the other with significant amounts of torsion.

The above qualitative discussion has presented a physical description of the VIRAS effect. Within the discussion, we have implicitly assumed the use of the Watson rotation-vibration Hamiltonian for a semi-rigid molecule, based upon the Eckart frame. Before presenting the formal treatment of the VIRAS effect for 2FE another aspect of angular momentum coupling is considered. The internal angular momentum generated by the large-amplitude torsional motion of the hindered rotor can couple to the overall rotation of the molecule. In order to develop a quantitative theory for 2FE, it is necessary to go beyond the Watson Hamiltonian and treat explicitly the coupling of large-amplitude torsional motion with overall rotation.

C. Coupling of Internal Rotation and Overall Rotation in 2-Fluoroethanol

In this subsection, we derive a Hamiltonian describing interaction of overall rotation with a single large-amplitude internal rotation coordinate.[26,27] The model Hamiltonian is then applied to describe the

interaction of rotation with internal rotation about the C-C bond in 2FE. Internal rotation about the C-O bond involves solely the motion of a hydrogen atom. The perturbation caused by this internal rotation is small in terms of the VIRAS effect and is assumed to be only weakly coupled to the overall rotation. Therefore, the C-O torsion is not considered explicitly, but is treated as an uncoupled hindered rotor. All remaining 3N-8 internal coordinates are treated as high frequency small amplitude vibrational coordinates. Although we shall not need to specify the precise choice of embedding for the molecule-fixed frame, the Eckart-Sayvetz frame[22] is a natural choice.

The coordinate system used is shown in Fig. 2. Note in particular that the internal rotor angle χ is half the FCCO torsion angle, so that internal rotation generates only a small amount of angular momentum about the C-C axis. In the treatment of the FCCO torsion, the OH group is a single point mass.

Following standard procedures[27], the quantum mechanical rotation-torsion Hamiltonian for the model of Fig. 2 is found to be:

$$H=\frac{1}{2}J\mu J + GP_{\chi}^{2} + \pi\mu\pi + V(\chi) - 2\pi\mu J \qquad \text{[Eq. 3]}$$

$$\mu = (I - \tilde{B}\frac{1}{D}B)^{-1}$$

$$B=\sum_{\alpha} m_{\alpha} r^{\alpha} \times \left(\frac{dr^{\alpha}}{d\chi}\right)$$

$$D=\sum_{\alpha} m_{\alpha}(\frac{dr^{\alpha}}{d\chi})^{2}$$

$$\pi=\tilde{B}\frac{1}{D}P_{\chi}$$

$$G=\frac{1}{D}$$

Here, $V(\chi)$ is the torsional potential, m^{α} and r^{α} are mass and position vectors of α-th atom. I is the inertia tensor, which varies with torsional angle χ.

H can be partitioned into three parts, corresponding to overall rotation, internal rotation and the interaction between internal rotation and overall rotation. The first term on the right hand side of Eq. 3 represents overall rotation, the second and fourth terms represent internal rotation and the third and fifth terms are interaction terms. Note that both the μ-tensor and the G coefficient depend on χ. The above Hamiltonian can be expanded and simplified to the form:

$$\begin{aligned} H=&\mu_{xx}J_x^2+\mu_{yy}J_y^2+\mu_{zz}J_z^2 \\ &+\mu_{xy}(J_xJ_y+J_yJ_x)+\mu_{xz}(J_xJ_z+J_zJ_x) \\ &+\mu_{yz}(J_yJ_z+J_zJ_y)+H_T \\ &-\frac{1}{2}[(RI_xJ_x+RI_yJ_y+RI_zJ_z)P_\chi \\ &+P_\chi(RI_xJ_x+RI_yJ_y+RI_zJ_z)] \end{aligned} \qquad \text{[Eq 4]}$$

$$RI_x=\frac{2}{D}(\mu_{xx}B^x+\mu_{xy}B^y+\mu_{xz}B^z)$$

$$RI_y=\frac{2}{D}(\mu_{xy}B^x+\mu_{yy}B^y+\mu_{yz}B^z)$$

$$RI_z=\frac{2}{D}(\mu_{xz}B^x+\mu_{yz}B^y+\mu_{zz}B^z)$$

In this form of the Hamiltonian we have made one further approximation: the χ dependence of G in the internal rotation part of the Hamiltonian is ignored. This modification is expected to have only a minor effect on the

results and greatly simplifies the calculation. The eigenfunctions of H_T are denoted $|m\rangle$, m=0,1,... . For a given J, rotation-torsion eigenfunctions are expanded as sums of products of symmetric rotor wavefunctions with torsional wave functions $|m\rangle$:

$$|\psi\rangle=\sum_K \sum_m C_m^K|J,K\rangle|m\rangle \qquad \text{[Eq. 5]}$$

The rotation-torsion component of the bright state associated with the vibrational transition of interest is taken to be a product of a rotational eigenfunction for an asymmetric top with appropriate rotational constants and the torsional ground state function $|m=0\rangle$. The bright state can also be expanded in the same product basis set used above:

$$|\phi\rangle=\sum_K D_K|J,K\rangle|m=0\rangle \qquad \text{[Eq. 6]}$$

The bright and dark states are now written as products of rotation-torsion states, expanded as above, with vibrational states for the 3N-7 remaining degrees of freedom. To estimate the number of dark states coupled to a given bright state, it is necessary to evaluate matrix elements of the form:

$$\langle\psi|\langle\{n_j\}|\dot{H_v}|v_{C\text{-}H}=1\rangle|\phi\rangle \qquad \text{[Eq. 7]}$$

where $\dot{H_v}$' is the term in the Hamiltonian representing the effect (direct and via higher order perturbations) of residual anharmonic interactions between the torsion-vibrational modes. The set of dark states contain vibrational states of very different character. At the energy of interest, a given dark state may correspond to excitation of only a few quanta of torsion, or as many as 70 or 80 quanta. The precise nature of the anharmonic perturbations which

couple states with such disparate numbers of quanta is unclear. From experiment, it is apparent that the density of coupled states far exceeds the number of available vibrational states. We therefore make the drastic assumption that *all available dark states in the vicinity of the bright state will couple, via an unknown anharmonic perturbation, with the bright state.* We further assume that the matrix elements of the anharmonic perturbation connecting the bright state $|m=0\rangle |\{n_i\}\rangle$ with any dark state $|m\rangle |\{n_f\}\rangle$ are *equal.* Using this approximation, the relative magnitudes of the coupling matrix elements become:

$$\langle\psi|\langle\{n_j\}|H_v'|v_{C\text{-}H}=1\rangle|\phi\rangle \sim \sum_K D_K \sum_m C_m^{K*} \langle m|H_v'|m=0\rangle \qquad \text{[Eq. 8]}$$

$$\sim \sum_K D_K \left(\sum_m C_m^{K*}\right)$$

where $\{C_{k,m}\}$ are the expansion coefficients of the torsional-rotational eigenstates in the $|J,K\rangle |m\rangle$ basis, and D_k are expansion coefficients of the bright state in the same $|J,K\rangle$ basis. Eq. 8 therefore expresses the magnitude of the coupling matrix element as a sum of overlaps of rotational components.

When the principal axes of a dark state do not coincide with those of the bright state, the bright state can in principle couple to the entire manifold of rotational states associated with the dark state as long as J is conserved. In practice, if the coupling matrix element is sufficiently small, a transition to that state would not be observed experimentally. Based on the experimental signal-to-noise ratio, we set the threshold overlap of dark states with bright states to be 1% of the maximum overlap, and further assume that any dark state having an overlap with the bright state above the threshold is detectable experimentally.

This procedure is demonstrated in detail for the case of 2FE in the next Section.

III. VIRAS AND 2-FLUOROETHANOL

Using the procedure outlined in the previous Section, we now calculate the density of states available for coupling in 2FE.

There are 21 normal modes in 2FE, of which two are torsional modes, corresponding to rotation about the C-C bond and the C-O bond, respectively. The fundamental frequencies of these modes have been measured and assigned experimentally.[25] In order to make a crude estimate of the vibrational density of states, we treat the 2 torsional modes separately as hindered rotors, while the other 19 modes are treated as uncoupled anharmonic oscillators.[6,7] A 2% anharmonicity is assumed for all modes. The potential functions for the two torsional modes are shown in Figure 3. The C-O torsional potential is a calculated function from the work of Wiberg and Murcko.[28] The C-C torsional potential was generated to correspond to experimentally determined values of the barrier heights and relative well depths. Direct counting of the vibrational states including a 2% anharmonicity then gives an average calculated density of states of 56 states/cm^{-1} at 2980 cm^{-1}. With anharmonic coupling alone, the maximum number of available states in this region is therefore 56/cm^{-1}. Both Coriolis coupling and the VIRAS mechanism can result in rovibrational mixing, thereby increasing the number of states available for coupling in this spectral region. We now calculate the number of coupled states using the VIRAS model of the previous Section.

A normal mode analysis of 2FE was performed using MOPAC[30]. The input geometry of 2FE was determined from experimental data.[25] MOPAC

excuted a MNDO[31] calculation on the input geometry until a stable geometry was found; only minor modifications to the input geometry resulted. The MNDO calculation also produced force constants, vibrational frequencies, normal modes, and the transformation matrix from cartesian coordinates to normal coordinates. The calculated frequencies from the normal mode analysis are in good agreement with experiment for the high frequency modes, but some discrepancies are found for the low frequency modes (See Table I). The normalized normal coordinate eigenvectors were used to calculate classical RMS displacements of each atom at a vibrational energy equal to the zero-point energy. Assuming an adiabatic separation of vibration and rotation, the geometry change upon excitation of the 19 small-amplitude harmonic modes is not sufficient to significantly rotate the principal axes in the molecule, so that VIRAS will not be important for these modes. Excitation of the torsional modes, however, results in much larger average displacements of the atoms in the molecule and possibly concomitant rotation of the principal axes. Torsion about the C-O bond has only a small effect on the inertial parameters of the molecule. The mass of the hydrogen is so small that changes in the inertia tensor as a function of C-O torsion angle are negligible. When calculating molecular geometries we therefore fix the torsional angle of the OH group along the C-O bond at 55.5°, based on the geometry from microwave experiments.[25]

Since there are such small changes in geometry upon excitation of vibrations other than the torsional modes, changes in inertial parameters due to excitation of these other modes are henceforth neglected. Excitation of the large-amplitude C-C torsion mode leads to the largest VIRAS effect, and we now consider the interaction of this mode with overall rotation.

The Hamiltonian describing interaction of rotation with large-amplitude C-C torsion was given in the previous Section. The torsional basis used consists of eigenstates of the torsional Hamiltonian H_T. The torsional potential for the C-C torsion was modelled as a periodic sum of cosines:

$$V=\frac{1}{2}\sum_n V_n(1-\cos(n\phi)) \qquad \text{[Eq. 9]}$$

where the V_n's are derived from experimental values for the barrier heights and relative well depths (See Figure 3).[28,29] The C-C torsional potential is shown in Figure 4, together with the energy levels determined for this potential. Torsional eigenfunctions were expanded as a sum of cosine and sine functions, and the expansion coefficients calculated based on the algorithm of Lewis et al.[26] The size of the expansion basis was increased until convergence within 0.2 cm^{-1} was attained. A representative selection of wavefunctions is shown in Figure 5. Note that V_{C-C} is a periodic function with two identical minima at the two gauche forms and a single local minimum at the Tt' form. The low energy torsional levels are nearly doubly degenerate with maximum probability density at the gauche forms. With increasing quantum number, new states appear with probability density at the trans form at approximately v=20. At higher quantum levels, the wavefunction begins to delocalize over all angular space (v>48).

A total of 120 torsional states are used in the expansion of the rotation-torsion eigenstates of Hamiltonian Eq. 4 From the coordinate system of Figure 2, it can be seen that the transformation $\chi \rightarrow \chi + 2\pi$ results in an overall rotation of the molecule by π about the C-C axis. The rotation-torsion basis functions must therefore satisfy the boundary condition:

$$\psi(\theta+\pi,\chi+2\pi)=\psi(\theta,\chi) \qquad \text{[Eq. 10]}$$

where θ is an Euler angle describing overall rotation about the C-C bond. Note that the full range of χ is $0 \rightarrow 4\pi$. Requiring the rotation-torsion eigenfunction to be single valued then implies that for an odd number of torsional quanta the K quantum number be odd, and for an even number of torsional quanta K must be even. For given J, a basis of 240 torsional states was used, half of which have the right symmetry to match even K states $|J,K\rangle$, the other half odd K. The set of basis functions consisting of the product of the $|J,K\rangle$ rotational states and the $|m\rangle$ torsional states is used to construct the rotation-torsion Hamiltonian matrix.

The Hamiltonian matrix is block diagonal in J, and each J block is diagonalized independently (for example, the J=5 block is 1320 x1320) to give rotation-torsion eigenvalues and eigenstates. The rotation-torsion states are combined with various other vibrations to form states of energy nearly resonant with the bright state. Such a combination state is shown schematically in Figure 6. The rotation-torsion component of the total eigenvectors can be projected onto the rotational bright states using Eq. 8. As discussed in the previous Section, to compare theory with experiment it is necessary to set a cutoff value for the overlap Eq. 8, below which the associated transition is deemed unobservable. This threshold is set at 1% of the maximum overlap. It should be emphasized that the 1% value is determined by the dynamic range of the experiment and is not an arbitrarily adjustable parameter.

The results of our quantum mechanical treatment of VIRAS in 2FE are shown in Figure 7 and presented in Table II. Many more rotational states associated with a single vibrational dark state are available to couple to a

given rotational level in the bright state than would be predicted from anharmonic coupling alone. For example, for J=4, the effective density of coupled states is increased from 56 states/cm^{-1} with anharmonic coupling alone to 276 states/cm^{-1}, as compared to the experimental measured value of 278 states/cm^{-1}. For the available experimental results, where J=0-5, our calculations are in very good agreement with the experimental data and well within the experimental uncertainties. The uncertainties in the experimental data are intrinsic to the physical quantity being measured, and therefore are not limited by the noise in the data.[7,8] The data suggests that there is mode-selectivity in the vibrational coupling that is not accounted for in the calculation. Mode-selective coupling results in differences in the magnitude of the coupling matrix elements for different vibrational dark states, and therefore different effective densities of states. The calculations presented here do not account for these differences because uniform coupling for different vibrational states is assumed.

The agreement between our model and the experiment has been achieved without any adjustable parameters. The precise nature of the dark states in the vicinity of a given bright state, however, is expected to be a sensitive function of the details of the torsional potential function. Although our potential function was constructed to agree with experimentally measured parameters, the form of the potential chosen is necessarily an approximation. To evaluate the effect of our choice of potential on the VIRAS predictions, we changed the barrier heights and relative well depths by 10% and recalculated the predicted density of coupled states. The results of this calculation are plotted as a function of J in Figure 8. These changes in the potential surface had only a small effect on the theoretical predictions, and our results remained in good agreement with the experimental data.

IV. CONCLUSION

The phenomenon of vibrationally induced rotational axis switching (VIRAS) has been proposed as a mechanism for explaining enhanced densities of coupled states in high-resolution spectra. VIRAS is a direct consequence of centrifugal distortion, and is best understood in terms of an adiabatic separation of vibrational and rotational motion. Each vibrational state has an effective rotational Hamiltonian obtained by averaging over the vibrational coordinates. The rotational constants and orientation of the principal axes will in general be different for each vibrational state, so that rotational eigenstates associated with different vibrational states are no longer orthonormal. The number of dark states to which a given bright state can be coupled by an anharmonic coupling term in the Hamiltonian is then increased due to nonzero "rotational Franck-Condon factors".

Application of the theory to 2FE showed that the C-C torsional mode exhibited the most pronounced VIRAS effect. An exact torsional-rotational Hamiltonian for 2FE was diagonalized to obtain rotation-torsion eigenstates for 2FE. Zeroth-order states were taken to be products of torsion-rotation states with vibrational states for the 3N-7 remaining modes. Assuming that anharmonic terms in the Hamiltonian couple every dark torsion-vibration state equally strongly to the bright torsion-vibration state, the coupling matrix element can be expressed as a sum of overlaps of rotational states. Using a reasonable threshold intensity for detection, we calculate the density of rovibrational states available for coupling. The theoretical predictions are found to be in good agreement with experiment.

Acknowledgement: This work is supported by: The National Institute of Health under grant #08-R9N527039A, The Office of Naval Research under grant #N00014-90-J-1971, and Proctor and Gamble (to LAP); and NSF grant CHE-9101357 (to GSE). GSE is a Camille and Henry Dreyfus Foundation Teacher-Scholar. The authors gratefully acknowledge S. W. Mork, C. L. Brummel, and M. Shen for generous help and stimulating discussion. We are particularly grateful to E.L. Sibert for his penetrating comments on an earlier version of this paper.

References

1. D.H. Levy, *Adv. Chem. Phys.* **47**, 323 (1981).

2. F.F. Crim, *Science*, **249**, 1387 (1990).

3. J.S. Baskin, M. Dantus, A.H. Zeweil, *Chem. Phys. Lett.* **130**, 473 (1983); P. Felker, A.H. Zewail,*Chem. Phys. Lett.* **102** 13 (1986); R.B. Bernstein, A. H. Zewail, *J. Chem Phys.* **90**, 829 (1989).

4. K.K. Lehmann, B.H. Pase and Scoles, *J. Chem. Phys.* 93, 2152 (1990).

5. A. McIlroy, D. Nesbitt, *J. Chem. Phys.* **91**, 104 (1990); **92**, 2229 (1990).

6. A.M. de Sonza, D. Kaur, D.S. Perry, *J. Chem. Phys.* **88**, 4569 (1988); **94**, 6153 (1990); J. Go, G.A. Bethardy, D.S. Perry, *J. Phys. Chem.* **94**, 6153 (1990).

7. C.L. Brummel, S.W. Mork, L.A. Philips, *J. Am. Chem. Soc.*, **113**, 4342 (1991).

8. C.L. Brummel, S.W. Mork, L.A. Philips, *J. Chem. Phys.*, **95**, 7041, (1991).

9. H.L. Dai, C.L. Korpa, J.L. Kinsey, R.W. Field, *J. Chem. Phys.* **82**, 1688 (1985).

10. J. Kommandeur, W.A. Majewski, W.L. Meerts, D.W. Pratt, *Ann. Rev. Phys. Chem.*, **38**, 433 (1987).

11. A. Knight, 1, in Excited States, Academic Press, Inc., (1988).

12. D.B. Moss, C.S. Parmenter, G.E. Ewing, *J. Chem. Phys.* **86**, 51 (1987).

13. C.S. Parmenter, B.M. Stone, *J. Chem. Phys.* **84**, 4710 (1986).

14. H.W. Schranz, L.M. Raff, D.L. Thompson, *Chem. Phys. Lett.*, **182**,455 (1991); R.H. Newman-Evans, R.J. Simon, B.K. Carpenter, *J. Org. Chem.*, **55**, 695 (1990); D.B. Borchardt, S.H. Bauer, *J. Chem. Phys.* **85**, 4980 (1983).

15. K.K. Lehmann, *J. Chem. Phys.*, **95**, 2361 (1991).

16. W.G. Harter, C.W. Patterson, *J. Chem. Phys.* **80**, 74 (1981).

17. M. Bixon, J. Jortner, *J. Chem. Phys.*, **48**, 715 (1968).

18. R.D. Levine, J. Jortner, 1, in Mode Selective Chemistry, B. Pullman *et al.*, ed., Reida, Dordredit, 1991.

19. T. Uzer, *Physics Reports* **199**, 73 (1991); A. Stuchebrukhov, S. Ionov and V. Letokhov, *J. Phys. Chem.*, **93**, 5357 (1982).

20. C.C. Martens, M.J. Davis and G.S. Ezra, *Chem. Phys. Lett.* **142**, 519 (1987); Y.M. Engel and R.D. Levine, *Chem. Phys. Lett.* **164**, 270 (1990).

21. C.C. Martens, W.P. Reinhardt, *J. Chem. Phys.*, **93**,5621 (1990).

22. D. Papousek, M.R. Aliev, Molecular Vibrational-Rotational Spectra, Elsevier Scientific Publishing Co., 1982.

23. J. Hawkins Meal, S.R. Polo, *J. Chem. Phys.*, **24**, 1126 (1956); **24**, 1119 (1956).

24. J.T. Hougen, J.K.G. Watson, *Can. J. Phys.*, **43**, 298 (1967).

25. K.S. Buckton, R. Azrak, *J. Chem. Phys.* **52**, 5652 (1970).

26. C.R. Quade, C.C. Lin, *J. Chem. Phys.* **38**, 540 (1963).

27. C.C. Lin , *Rev. Mod. Phys.* **31**, 841 (1959).

28. J.W. Lewis, T.B. Malloy, Jr., T.H. Chao, J. Laane, *J. Mol. Struct.* **12**, 427 (1972).

29. K.B. Wiberg and M.A. Murcko, *J. Mol. Struct.* **163**, 1 (1988).

30. J.J.P. Stewart, *J. Comput -Aided Mol. Design* **4**, 1 (1990).

31. M.J.S. Dewar and D.W. Thiel, *J. Am. Chem. Soc.* **99**, 4899 (1977).

Figure Captions

Figure 1: Two examples of the relative orientation of the principal axes of the bright state and a particular dark state are shown. In part a, the dark state contains no torsion and there is little difference in the axes or the rotational constants for the two vibrational states. The dark state is composed of 1 quanta of V_6 and 1 quanta of V_{10} . In contrast, in part b, the dark state contains torsion and there is substantial reorientation of the principal axes and concomitant change in the rotational constants. There are 74 quanta of torsion in this dark state, well as 1 quanta of V_{16} and 1 quanta of V_{19}.

Figure 2: The axis system used to define the geometry of 2-fluoroethanol is presented. The angle χ is half of the FCCO dihedral angle.

Figure 3: The torsional potential functions for the C-C torsion and the C-O torsion are shown above. The C-O potential function was calculated at the MP3/6-311++G** level by Wiberg and Murcko[29] For the C-O torsion, the geometry about the C-C bond was held at the trans conformation. The C-C torsional potential was generated by a sum of cosines to correspond to experimentally determined values of the barrier heights and relative well depths.

Figure 4 : The energy levels for the C-C torsional potential are shown for energy levels up to v=50. There are three kinds of energy levels. There are symmetric and antisymmetric levels that are generated from the two identical

gauche potential wells, and levels corresponding to wavefunctions that have their maximum amplitude in the trans potential well.

Figure 5: The corresponding wavefunctions for a representative selection of the energy levels from Figure 4 are shown.

Figure 6: Shown schematically is an example of the relative energies of the bright state and a dark state containing 1 quanta of V_6 and 1 quanta of V_{10}, and the manifold of the states ψ_i determined from the diagonalization of the rotation-torsion Hamiltonian given in Equation 4 and described in the text.

Figure 7: Shown above is a plot of the density of coupled states versus the quantum number J for the experimental data from the spectrum of 2FE and two different coupling models. Squares: experimental data (dotted lines represent the experimental uncertainties); Triangles: the prediction of the VIRAS coupling model.

Figure 8: The plot shown is identical to the plot in Figure 7, except that the relative well depths and potential barriers for the C-C torsion potential were decreased by 10%. Note that with this substantial change in the potential, there remains good agreement between the VIRAS predictions and the experimental results.

Tables

Table 1: The vibrational modes in 2FE. The calculated frequencies are from the normal mode calculations. The assignments are from the experiments of R. Azrak and K.S. Buckton[25].

Table 2: The density of states as predicted by the VIRAS coupling model, as a function of the rotational quantum number, J.

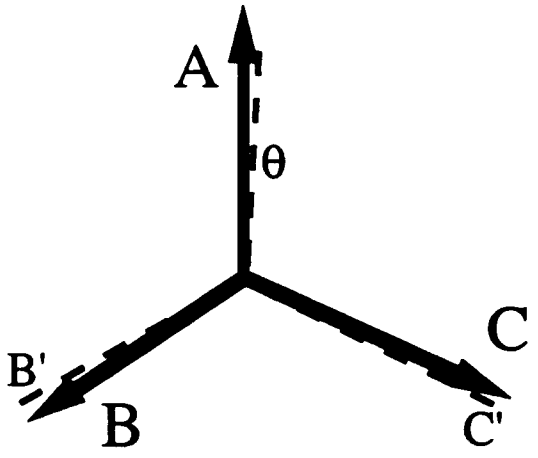

$A' = 0.5318\ cm^{-1}$
$B' = 0.1816\ cm^{-1}$
$C' = 0.1513\ cm^{-1}$

a

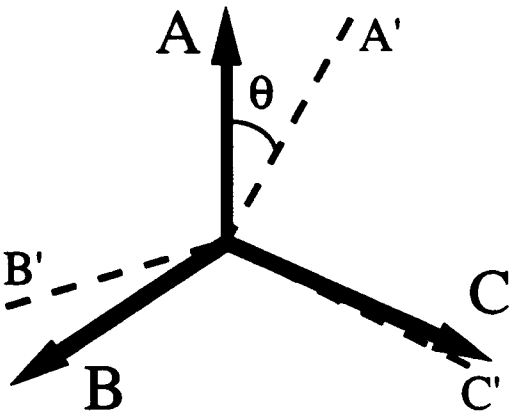

$A' = 0.5621\ cm^{-1}$
$B' = 0.1708\ cm^{-1}$
$C' = 0.1485\ cm^{-1}$

b

C-H Stretch

$A = 0.5317\ cm^{-1}$
$B = 0.1816\ cm^{-1}$
$C = 0.1513\ cm^{-1}$

Fig 1

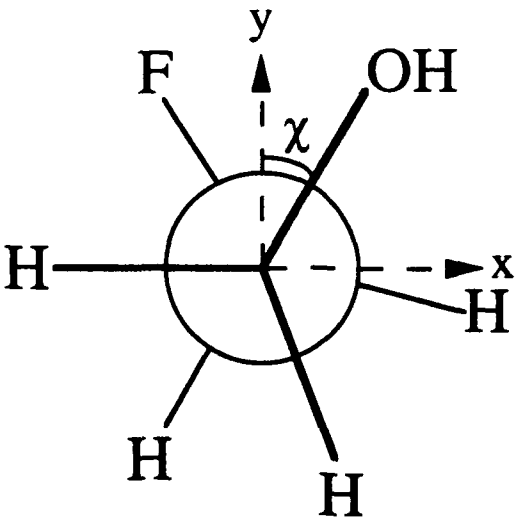

Fig 2

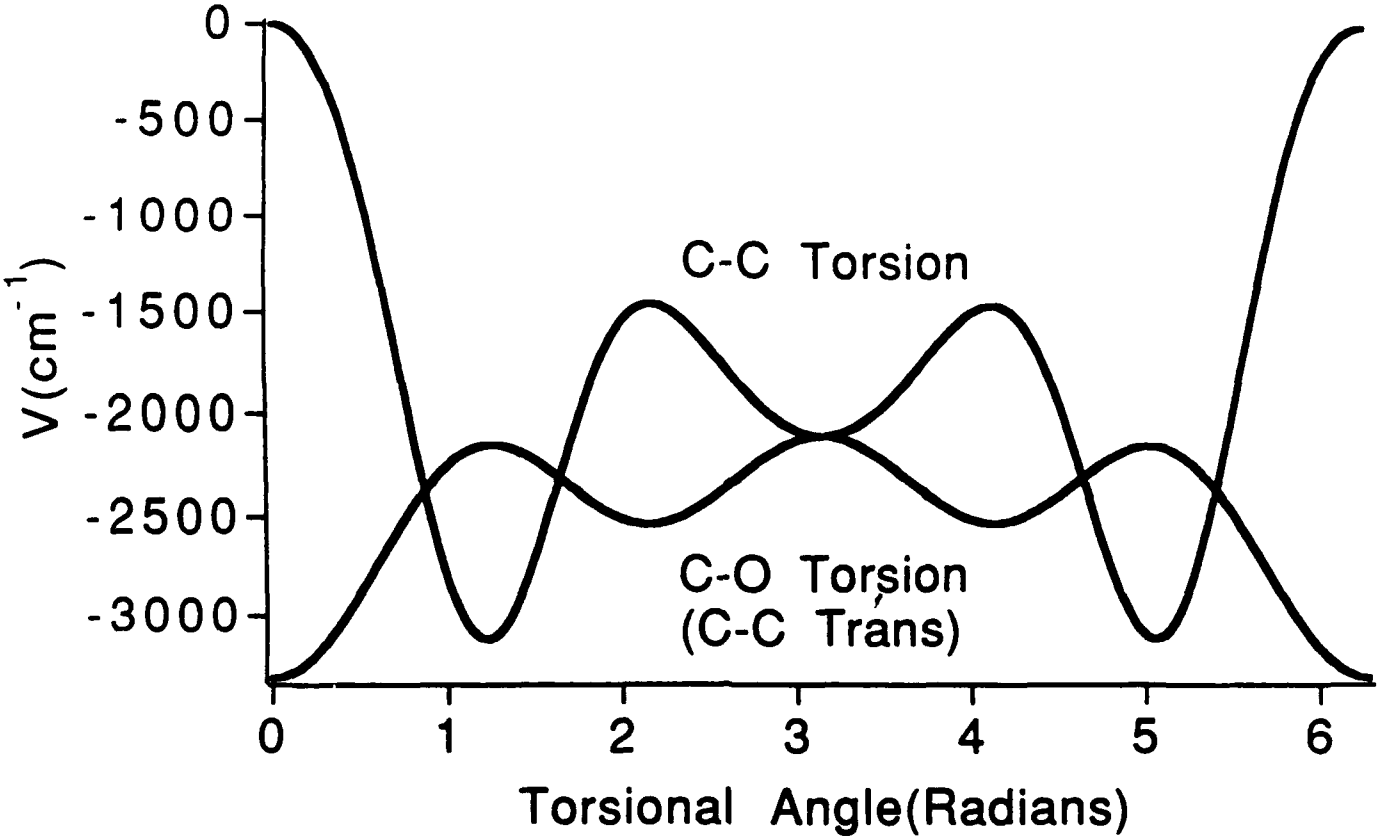
0
-500
-1000
-1500
-2000
-2500
-3000
V(cm^{-1})
C-C Torsion
C-O Torsion
(C-C Trans)
0
1
2
3
4
5
6
Torsional Angle(Radians)

Fig 3

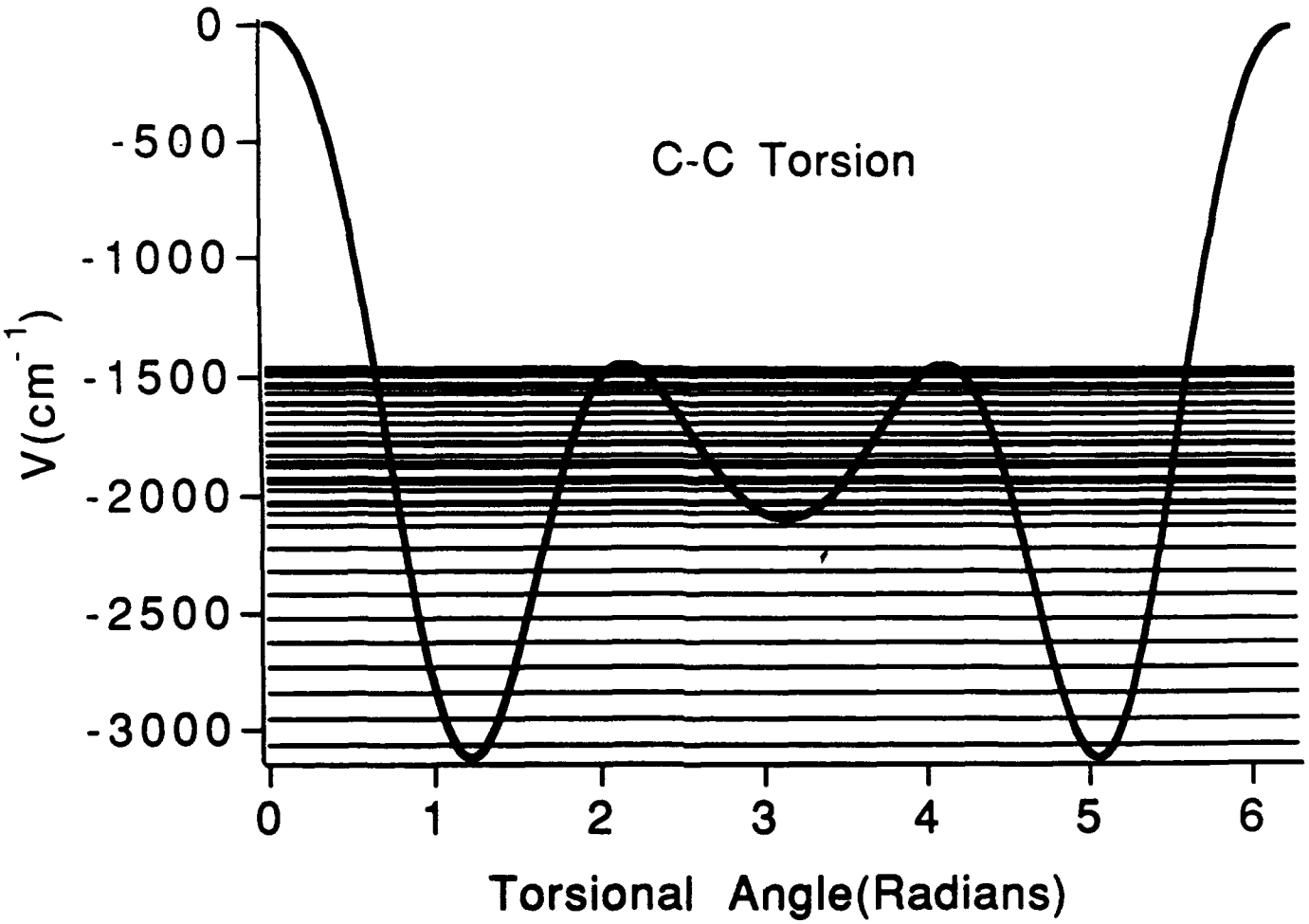
C-C Torsion
0
-500
-1000
-1500
-2000
-2500
-3000
V(cm-1)
0
1
2
3
4
5
6
Torsional Angle(Radians)

Fig 4

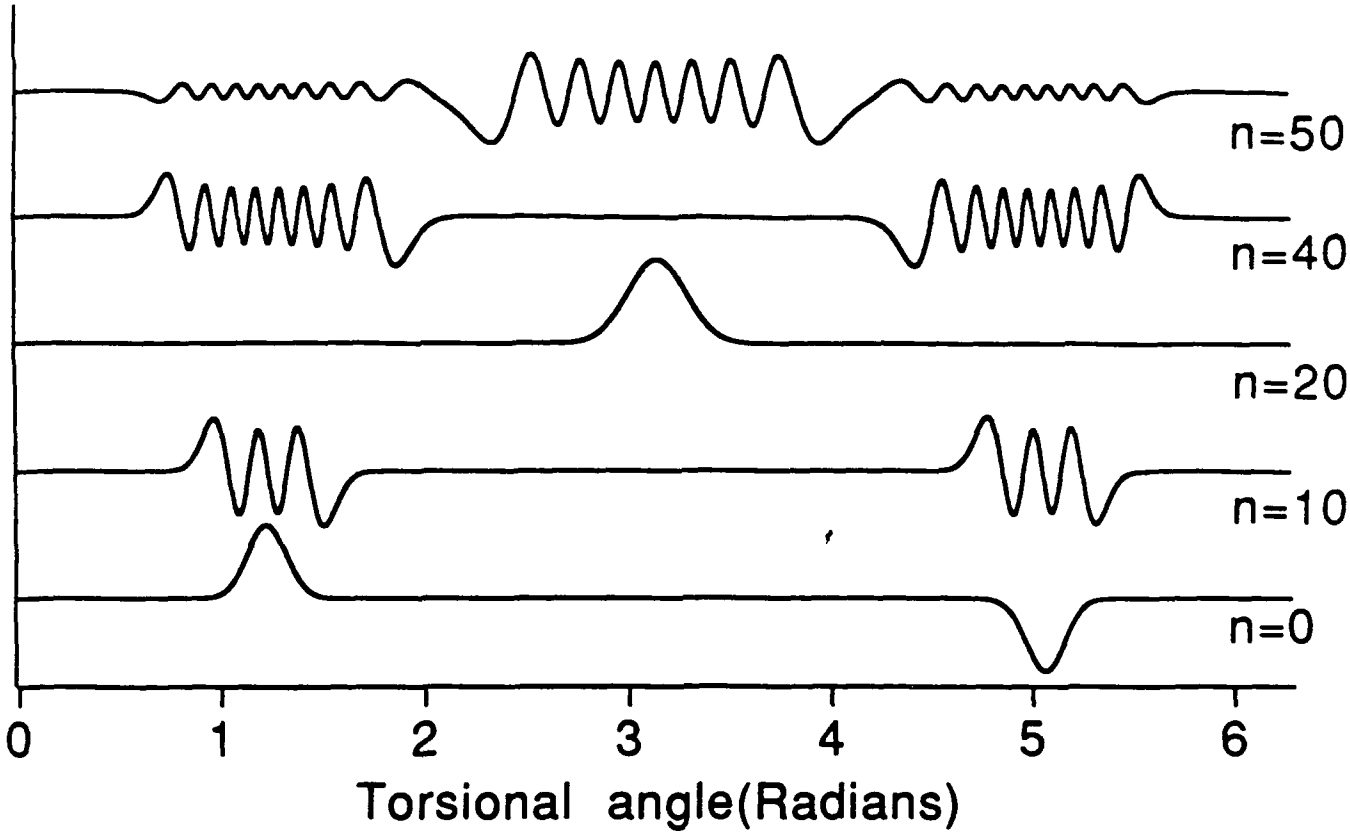

Fig 5

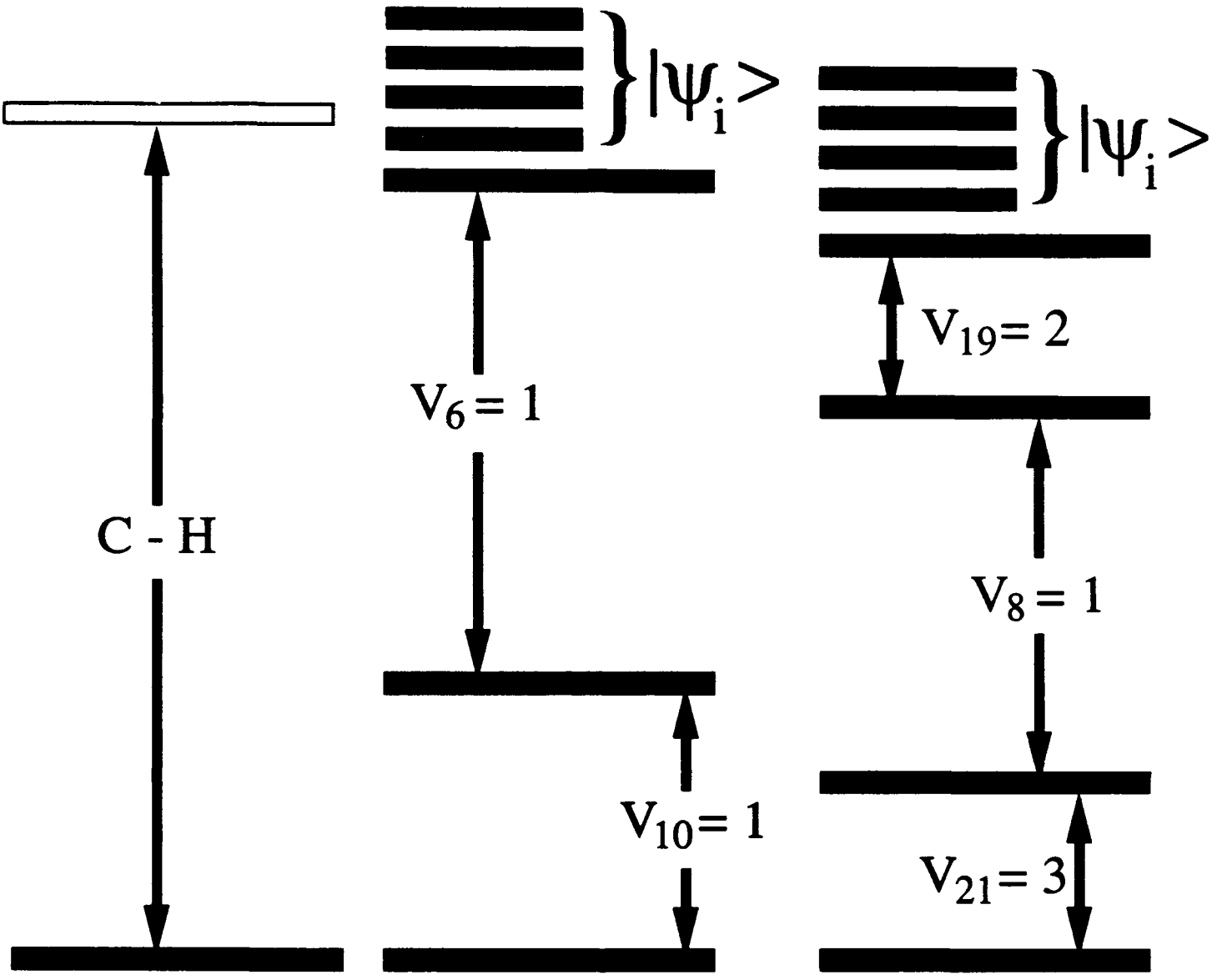

Fig 6

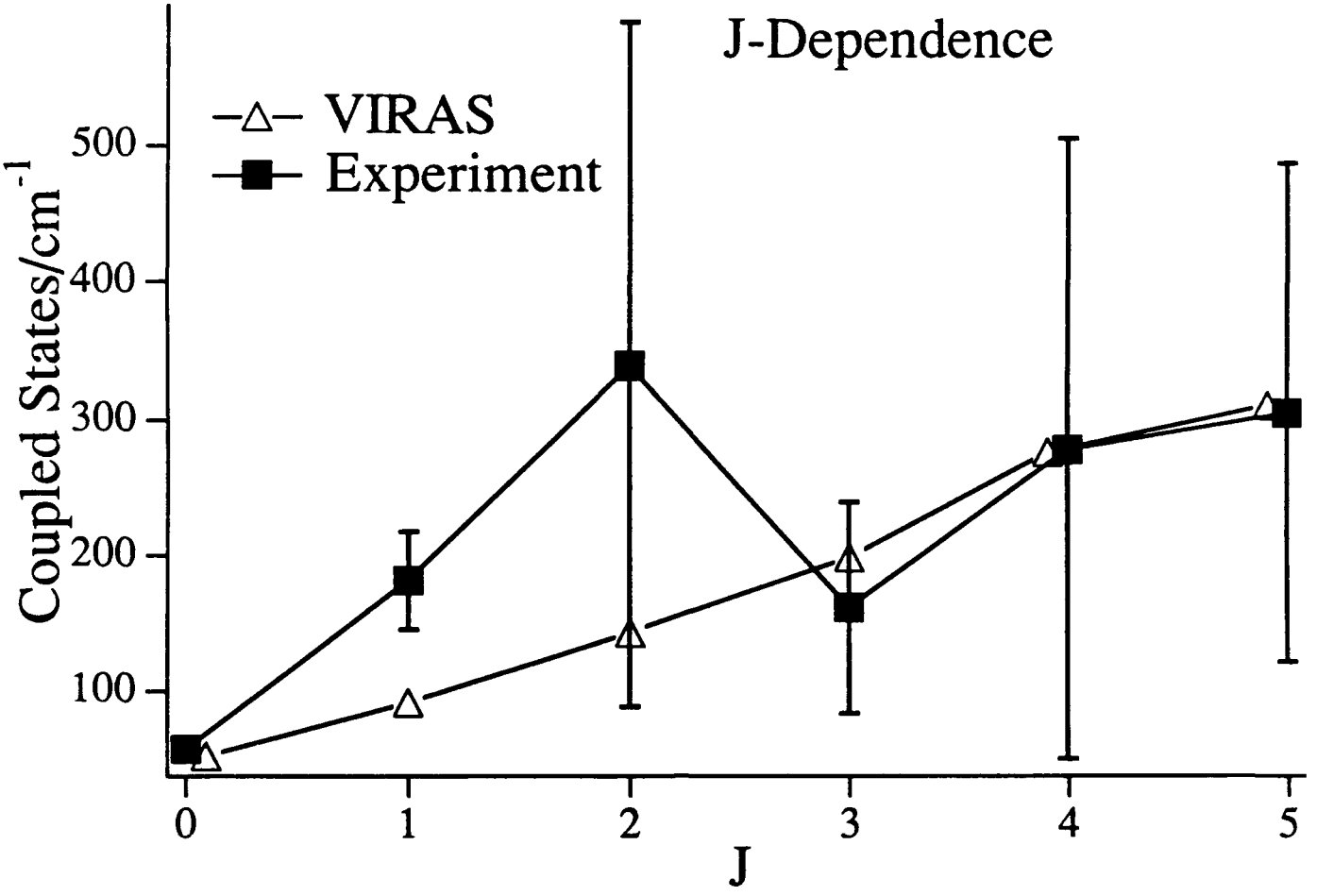
J-Dependence
VIRAS
Experiment
Coupled States/cm-1
500
400
300
200
100
0
1
2
3
4
5
J

Fig 7

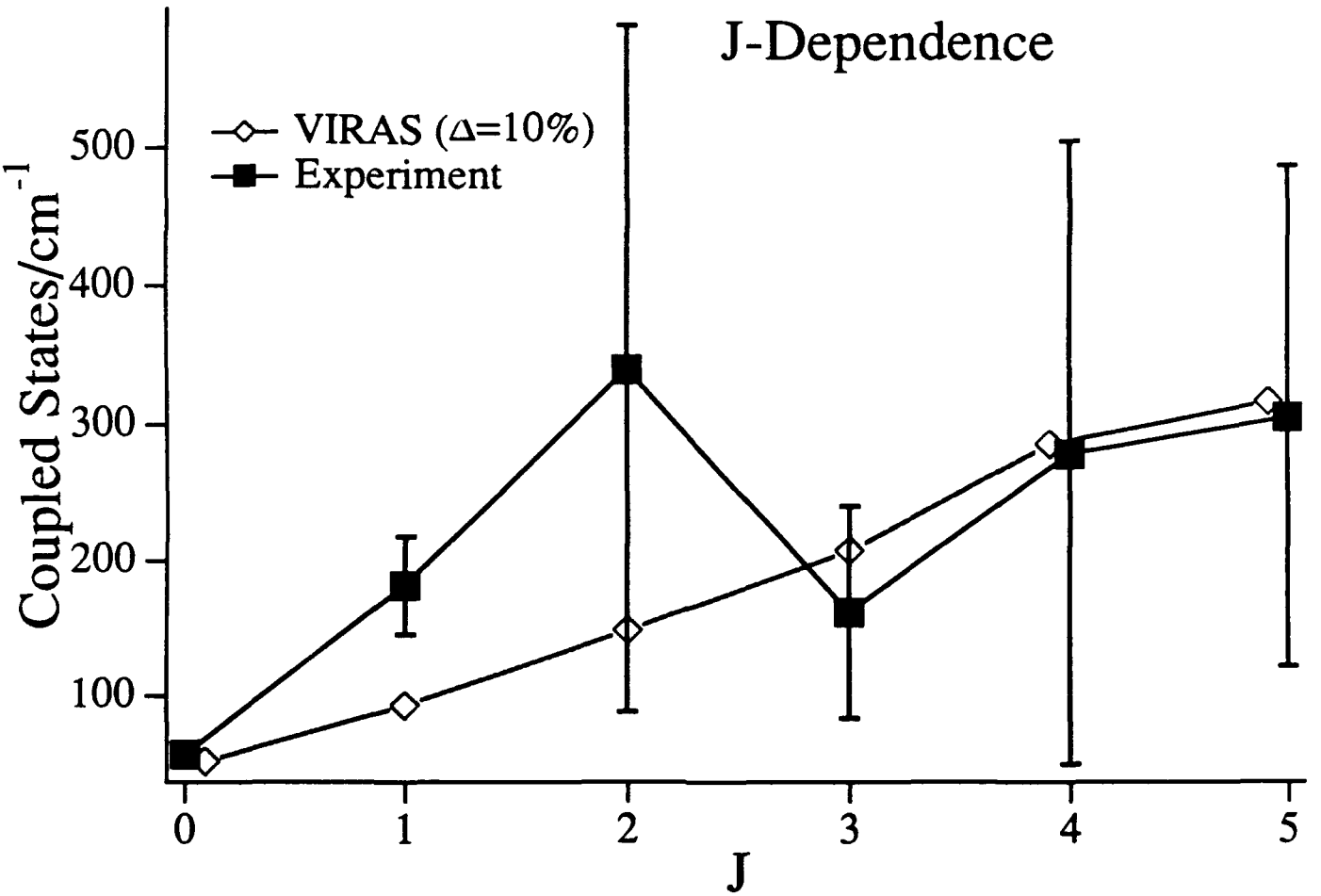
J-Dependence
VIRAS (Δ=10%)
Experiment
Coupled States/cm-1
500
400
300
200
100
0
1
2
3
4
5
J

Fig 8

υ	Observed(cm^{-1})	Calculated(cm^{-1})	Assignment
1	3626	3998	υOH
2	2980	3256	υ_aCH
3	2961	3248	υ_aCH
4	2926	3197	υ_SCH
5	2896	3185	υ_SCH
6	1460	1597	δ_SCH
7	1458	1544	ωCH
8	1400	1513	ωCH
9	1373	1452	δ_SCH
10	1348	1430	tCH
11	1252	1425	tCH
12	1203	1400	δ_SHOC
13	1103	1315	υ_aOCC
14	1080	1241	υ_SOCC
15	1026	1124	υCF
16	885	1010	rCH,υ_SCCF
17	850	948	rCH
18	513	581	δOCC,CCF in phase
19	342	345	δOCC,CCF,out phase
20	292	289	τCOH
21	161	122	τFCCO

J	Density of States (per wave number)
0	51.70
1	91.40
2	142.9
3	198.4
4	276.1
5	310.6

TECHNICAL REPORT DISTRIBUTION LIST - GENERAL

Office of Naval Research (2)*
Chemistry Division, Code 1113
800 North Quincy Street
Arlington, Virginia 22217-5000

Dr. James S. Murday (1)
Chemistry Division, Code 6100
Naval Research Laboratory
Washington, D.C. 20375-5000

Dr. Robert Green, Director (1)
Chemistry Division, Code 385
Naval Air Weapons Center
Weapons Division
China Lake, CA 93555-6001

Dr. Elek Lindner (1)
Naval Command, Control and Ocean
Surveillance Center
RDT&E Division
San Diego, CA 92152-5000

Dr. Bernard E. Douda (1)
Crane Division
Naval Surface Warfare Center
Crane, Indiana 47522-5000

Dr. Richard W. Drisko (1)
Naval Civil Engineering
Laboratory
Code L52
Port Hueneme, CA 93043

Dr. Harold H. Singerman (1)
Naval Surface Warfare Center
Carderock Division Detachment
Annapolis, MD 21402-1198

Dr. Eugene C. Fischer (1)
Code 2840
Naval Surface Warfare Center
Carderock Division Detachment
Annapolis, MD 21402-1198

Defense Technical Information
Center (2)
Building 5, Cameron Station
Alexandria, VA. 22314

* Number of copies to forward